



# Energy dissipation and enstrophy production/destruction at very low Reynolds numbers in the final stage of the transition period of decay in grid turbulence

Cite as: Phys. Fluids **33**, 035147 (2021); <https://doi.org/10.1063/5.0041929>

Submitted: 27 December 2020 • Accepted: 26 February 2021 • Published Online: 23 March 2021

 Y. Zheng (鄭玉霖),  K. Nagata (長田孝二) and  T. Watanabe (渡邊智昭)



View Online



Export Citation



CrossMark

## ARTICLES YOU MAY BE INTERESTED IN

[Wavelet analysis of shearless turbulent mixing layer](#)

Physics of Fluids **33**, 025109 (2021); <https://doi.org/10.1063/5.0038132>

[Voronoi analysis of vortex clustering in homogeneous isotropic turbulence](#)

Physics of Fluids **33**, 035138 (2021); <https://doi.org/10.1063/5.0039850>

[Turbulence cascade model for viscous vortex ring-tube reconnection](#)

Physics of Fluids **33**, 035145 (2021); <https://doi.org/10.1063/5.0040952>

Physics of Fluids

SPECIAL TOPIC: Flow and Acoustics of Unmanned Vehicles

Submit Today!



# Energy dissipation and enstrophy production/destruction at very low Reynolds numbers in the final stage of the transition period of decay in grid turbulence

Cite as: Phys. Fluids **33**, 035147 (2021); doi: 10.1063/5.0041929

Submitted: 27 December 2020 · Accepted: 26 February 2021 ·

Published Online: 23 March 2021



Y. Zheng (鄭玉霖), K. Nagata (長田孝二), and T. Watanabe (渡邊智昭)

## AFFILIATIONS

Department of Aerospace Engineering, Nagoya University, Furo-cho, Chikusa, Nagoya 464-8603, Nagoya, Japan

<sup>a)</sup> Author to whom correspondence should be addressed: [nagata@nagoya-u.jp](mailto:nagata@nagoya-u.jp)

## ABSTRACT

Decay characteristics of turbulent kinetic energy and enstrophy in grid turbulence have been investigated in the far downstream region ( $x/M \sim 10^3$ :  $x$  is the downstream distance from the grid,  $M$  is the mesh size of the grid) through wind tunnel experiments using hot-wire anemometry, with the lowest turbulent Reynolds number  $Re_\lambda \approx 5$ . The non-dimensional dissipation rate  $C_\varepsilon$  increases rapidly toward the final stage of the transition period of decay and the profile agrees well with previous direct numerical simulation [W. D. McComb *et al.*, “Taylor’s (1935) dissipation surrogate reinterpreted,” Phys. Fluids **22**, 061704 (2010)] and theoretical estimation [D. Lohse, “Crossover from high to low Reynolds number turbulence,” Phys. Rev. Lett. **73**, 3223 (1994)] at very low  $Re_\lambda$  in decaying and stationary isotropic turbulence. The present result of  $C_\varepsilon$  is an update on the experimental data in grid turbulence toward a very low  $Re_\lambda$ , where measurements have been absent. The energy spectrum in the dissipation range at very low  $Re_\lambda$  deviates from a universal form observed at high Reynolds numbers. The decay rate of enstrophy is proportional to  $S + 2G/Re_\lambda$  ( $S$  is the skewness of the longitudinal velocity derivative and  $G$  is the destruction coefficient). It is shown that  $G$  and  $S + 2G/Re_\lambda$  increase rapidly with decreasing  $Re_\lambda$  at very low  $Re_\lambda$ , indicating that the effect of enstrophy destruction is dominant in the final stage of the transition period of decay. The profiles of  $S + 2G/Re_\lambda$  against  $Re_\lambda$  is well fitted by a power-law function even in the final stage of the transition period of decay.

Published under license by AIP Publishing. <https://doi.org/10.1063/5.0041929>

## I. INTRODUCTION

Homogeneous isotropic turbulence (HIT) is one of the most fundamental turbulences which has been extensively investigated by theories, direct numerical simulations (DNSs), and wind tunnel experiments using grid turbulence.<sup>1–5</sup> In these, the variations of turbulent kinetic energy (TKE) and enstrophy during the development and decay process have been matters of interest. The quite simplified but significant description using the longitudinal component of the double and triple correlation function,  $f$  and  $k$ , in HIT is derived from the Kármán–Howarth (K–H) equation<sup>6,7</sup>

$$\frac{\partial(fu_{\text{rms}}^2)}{\partial t} - u_{\text{rms}}^3 \left( \frac{\partial k}{\partial r} + \frac{4}{r}k \right) = 2\nu u_{\text{rms}}^2 \frac{\partial}{\partial r} \left( \frac{\partial f}{\partial r} + \frac{4}{r}f \right), \quad (1)$$

where  $t$  is the time,  $u_{\text{rms}}$  is the root mean square (rms) of velocity fluctuations,  $r$  is the separation of the two-point, and  $\nu$  is the kinematic viscosity. The longitudinal components of  $f$  and  $k$  are defined as

$$f(r) = \frac{\overline{u(x)u(x+r)}}{\overline{u^2(x)}}, \quad (2)$$

$$k(r) = \frac{\overline{u^2(x)u(x+r)}}{\overline{u^3(x)}}, \quad (3)$$

where  $u$  is the velocity fluctuation in the  $x$  direction and  $\bar{\cdot}$  denotes the ensemble average (or time average in the experiment) of  $\cdot$ . The K–H equation is of great importance since equations related to the velocity and vorticity fields can be deduced by assuming large and small  $r$  in Eq. (1). The time variation of velocity and vorticity fluctuations is given by<sup>3</sup>

$$\frac{3}{2} \frac{du_{\text{rms}}^2}{dt} = -\varepsilon, \quad (4)$$

$$\frac{d\omega_{\text{rms}}^2}{dt} = -\frac{7}{3\sqrt{15}} \omega_{\text{rms}}^3 (S + 2G/Re_\lambda), \quad (5)$$



where  $\varepsilon$  is the dissipation rate of TKE,  $\omega_{\text{rms}}$  is the rms of vorticity fluctuations,  $S$  is the skewness of the longitudinal velocity derivative,  $G$  is the destruction coefficient of vorticity, and  $Re_\lambda = u_{\text{rms}}\lambda/\nu$  ( $\lambda = u_{\text{rms}}/\{(\partial u/\partial x)^2\}^{1/2}$  is the Taylor microscale) is the turbulent Reynolds number.  $S$  and  $G$  are given by

$$S = \frac{\overline{\left(\frac{\partial u}{\partial x}\right)^3}}{\left[\overline{\left(\frac{\partial u}{\partial x}\right)^2}\right]^{3/2}}, \quad (6)$$

$$G = u_{\text{rms}}^2 \frac{\overline{\left(\frac{\partial^2 u}{\partial x^2}\right)^2}}{\left[\overline{\left(\frac{\partial u}{\partial x}\right)^2}\right]^2}. \quad (7)$$

Since grids with various geometries placed in a uniform flow can generate quasi HIT, they have been used for wind tunnel experiments for many decades. It has been broadly accepted that when large-scale self-similarity exists in grid turbulence, the dissipation rate of TKE is expressed as<sup>8,9</sup>

$$\varepsilon = \frac{C_\varepsilon u_{\text{rms}}^3}{L}, \quad (8)$$

where  $C_\varepsilon$  is the non-dimensional dissipation rate and  $L$  is the integral length scale. In experiments of grid turbulence, the following power-law decay form is broadly accepted to investigate the decay of TKE:<sup>4,10–13</sup>

$$\frac{u_{\text{rms}}^2}{U^2} = a \left( \frac{x}{M} - \frac{x_0}{M} \right)^{-n}. \quad (9)$$

Here,  $U$  is the mean velocity,  $a$  is the decay coefficient,  $x$  is the downstream distance from the grid,  $x_0$  is the virtual origin,  $M$  is the grid mesh size, and  $n$  is the decay exponent. Richardson–Kolmogorov cascade states that Eq. (8) with a constant value of  $C_\varepsilon$  is valid at sufficiently high  $Re_\lambda$  and many previous investigations proved that  $C_\varepsilon$  is almost constant in grid turbulence from moderate to high turbulent Reynolds numbers.<sup>2,9,10,14</sup> However, at a low turbulent Reynolds number, where the viscous effects are predominant and the essential prerequisites of the Richardson–Kolmogorov cascade are broken down,  $C_\varepsilon$  is no longer constant. So far, the conclusive value of  $C_\varepsilon$  has not experimentally shown at very low turbulent Reynolds numbers although numerical and theoretical estimations have been made for decaying<sup>5</sup> and stationary<sup>15</sup> isotropic turbulence.

Nevertheless, Batchelor and Townsend<sup>16</sup> explicitly described that the TKE decay process of HIT includes the initial and final period, in which different decay exponents exist. Based on the conservation of Loitsyansky's integral with a constant  $C_\varepsilon$ ,  $n = 10/7$  in the initial period and  $n = 5/2$  in the final period are demanded, and this type of turbulence is referred to as Batchelor turbulence.<sup>10,17</sup> Later, Bennett and Corrsin<sup>18</sup> conducted a similar study of decaying turbulence and confirmed that the initial and final period of the TKE decay behaved as Batchelor turbulence. However, in accordance with the conservation of Saffman's integral with a constant  $C_\varepsilon$ , Saffman<sup>11</sup> deduced that  $n = 6/5$  in the initial period and  $n = 3/2$  in the final period, and this type of turbulence is referred to as Saffman turbulence. Skrbek and Stalp<sup>19</sup> reanalyzed the experimental data of Bennett and Corrsin<sup>18</sup> with the same manner as that in Batchelor and Townsend<sup>16</sup> and claimed that the data in the final period of decay at  $Re_\lambda \approx 4$  and  $x/M > 500$  is consistent with  $n = 3/2$  instead of  $n = 5/2$ , which

supported that the decaying grid turbulence is of Saffman type. Although the K–H equation is simplified in the final period of decay due to vanishing of the nonlinear effect, Djenidi *et al.*<sup>20</sup> indicated that most previous grid-turbulence experiments are performed in the transition period of decay (between the initial and final period) and it would be difficult to reach the final period of decay in the wind tunnel experiments due to the limitation of apparatus and relative increase in signal-to-noise ratio in the far downstream region.

On the other hand, for the variations of enstrophy in grid turbulence, the derivative skewness  $S$  is the surrogate of the rate of the production of enstrophy through the stretching of vortex filaments, while the destruction coefficient  $G$  represents the rate of destruction of enstrophy due to viscosity.<sup>3,21</sup> Physically,  $S$  is negative and  $G$  is positive in turbulent flows. Kolmogorov<sup>10</sup> argued that  $S$  remains constant, while he made an additional explanation considering the small-scale intermittency that  $S$  depends on  $Re_\lambda$ .<sup>22</sup> Since then, experimental investigations of  $S$  have been made in different kinds of flows.<sup>18,23–26</sup> Despite the extensive work on the behavior of  $S$ , variations of enstrophy (including  $S$  and  $G$ ) during the decay process need to be clarified, especially in the transition or the final period of decay.

The objective of the present study is to investigate the non-dimensional dissipation rate of TKE and enstrophy production/destruction in grid turbulence in the final stage of the transition period of decay. In particular, we focus on the behavior of  $C_\varepsilon$  from moderate to very low  $Re_\lambda$ . Besides, measurements of  $S$  and  $G$  are conducted to understand the variations of enstrophy during the decay process. The measurement of  $C_\varepsilon$ ,  $S$ , and  $G$  (or  $S + 2G/Re_\lambda$  appearing in the enstrophy equation) at very low  $Re_\lambda$  has not been reported and the present study offers updated profiles for  $Re_\lambda$  dependence of these quantities.

This paper is organized as follows: In Sec. II, we briefly describe the wind tunnel, grids for generating turbulence, and measurements. Section III shows the decay characteristics of turbulent intensities, dissipation, spectra, and variations of quantities related to enstrophy. Finally, Sec. IV summarizes conclusions.

## II. EXPERIMENTAL SETUP

The experiments are performed in an open-type wind tunnel at Nagoya University. The test section has a  $0.6 \times 0.6 \text{ m}^2$  cross section, and its length is 12 m. The top walls of the test section are made of acrylic resin and others are made of glass. The contraction ratio of the wind tunnel is 9 : 1. A turbulence-generating grid is installed at the entrance to the test section. The coordinate system is expressed in  $x$ ,  $y$ , and  $z$  coordinates, which describe streamwise, vertical, and lateral directions, respectively. The origin is located at the center of the grid.

The grids with different geometrical characteristics (i.e., biplane square, single-plane square, and woven-mesh grids) are used (Fig. 1). The mesh sizes of the grids are  $M = 5, 10, 15$ , and 50 mm and the solidity of the grid is 0.36 except  $M = 5 \text{ mm}$  grid, whose solidity is 0.39. These values are typical for grid-turbulence experiments.<sup>2,4,12,13,20,27</sup> The details of the grids are summarized in Table I.

Instantaneous streamwise velocity is measured using constant-temperature hot-wire anemometry (Dantec Dynamics, Streamline) with an I-type probe (Dantec Dynamics, 55P11). The I-type probe is used because of the smaller spatial resolution than an X-type one for accurately estimating derivative statistics. The length of the probe is 1.25 mm and its diameter is  $5 \mu\text{m}$ , so that the aspect ratio is 250. The overheat ratio is set to 0.8. The signal is amplified by a signal



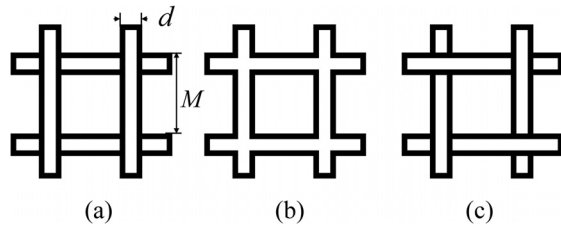


FIG. 1. Schematic of (a) biplane square, (b) single-plane square, and (c) woven-mesh grids.

conditioner and then recorded and sent to the personal computer from the A/D converter (National Instruments, NI-9215). A standard pitot tube is used to calibrate the hot-wire probe in the wind tunnel with a small background turbulent intensity. At low wind speed, the output voltage from the probe does not follow the King's law. Thus, we use the fourth-order polynomial fit in the calibration, where all  $U_0$  are covered.

The experiments are conducted five times at each downstream location to obtain reliable statistics. The scatter among five experiments is shown in each figure with uncertainty bars showing the standard deviation. The measurements are conducted on the centerline of the test section from  $x = 0.8$  m to 5.8 m, beyond which the increased boundary layer thickness and generation of secondary flows at the corner may affect the measurements on the centerline. The sampling number and frequency are set to 524 288 and 20 kHz, respectively, aiming to acquire reliable statistics. The eighth-order Butterworth low-pass filter is applied to the time series of data to remove the high-frequency noise inevitably contained in the signal. The cutoff frequency is set at the minimum of dissipation spectrum, where the small-scale characteristics are beginning to be polluted by the electronic noise.

Table II summarizes the experimental conditions. Inlet velocity  $U_0$  varies 2–10 m/s and mesh Reynolds number  $Re_M (= U_0 M / \nu)$  varies 680–33 000. Values of  $Re_\lambda$  are also included in Table II.

### III. RESULTS AND DISCUSSIONS

#### A. Decay of turbulent intensity

Figure 2 shows the streamwise variations of relative turbulent intensity  $u_{rms}^2 / U^2$  with streamwise distance from a virtual origin  $x_0$ , according to Eq. (9). It is shown that the power-law decay along the streamwise direction can be seen for all cases. The overall background turbulent intensity  $u_{rms} / U$  is less than or comparable to 0.06%, which is similar to 0.04% in Makita.<sup>29</sup> The maximum decay range method,<sup>4</sup> regression method,<sup>2,12,28</sup> regression method with zero virtual origins, and maximum decay range method based on  $\lambda^{20}$  are used to calculate

TABLE I. Geometrical characteristics of grids. Here,  $d$  is the thickness of the grid bars.

| Grid | $M$ (mm) | $d$ (mm) | Solidity $\sigma$ | Shape                 |
|------|----------|----------|-------------------|-----------------------|
| M50  | 50       | 10       | 0.36              | Square (biplane)      |
| M15  | 15       | 3        | 0.36              | Square (biplane)      |
| M10  | 10       | 2        | 0.36              | Square (single-plane) |
| M5   | 5        | 1.1      | 0.39              | Woven-mesh            |

TABLE II. Experimental conditions and flow parameters.

| Symbol                    | $M$ (mm) | $U_0$ (m/s) | $Re_M$ | $Re_\lambda$ | $n$             |
|---------------------------|----------|-------------|--------|--------------|-----------------|
| Square (green)            | 50       | 10          | 33 000 | 76–114       | $1.19 \pm 0.05$ |
| Circle (red)              | 15       | 10          | 9600   | 40–47        | $1.23 \pm 0.03$ |
| Up triangle (dark yellow) | 15       | 6           | 5800   | 25–33        | $1.28 \pm 0.03$ |
| Cross (blue)              | 15       | 4           | 3900   | 20–29        | $1.39 \pm 0.04$ |
| Diamond (purple)          | 10       | 2           | 1300   | 11–15        | $1.41 \pm 0.05$ |
| Left triangle (magenta)   | 5        | 2           | 680    | 5–7          | $1.45 \pm 0.02$ |

$n$  in Eq. (9). Generally, different methods yield the similar value of  $n$  and the range of  $n$  with the mean values are listed in Table II. It should be noted that the decay exponent is insensitive to  $x_0$  in the far field where  $x$  is large as in present study.

Figure 3 shows the streamwise variations of  $Re_\lambda$ .  $Re_\lambda$  decays slowly along the streamwise direction at large  $x/M$ , and very long streamwise distance will be required to achieve very small value of  $Re_\lambda$ , which is consistent with Djenidi *et al.*<sup>20</sup>

Variations of  $n$  vs  $Re_\lambda$  are compared with previous studies in Fig. 4. The minimum value of  $Re_\lambda$  in each case in Table II is used<sup>20</sup> for plots in Fig. 4. The dashed and solid lines represent the eddy-damped quasi-normal Markovian (EDQNM) results for Batchelor and Saffman turbulence in different periods of decay.<sup>30</sup> Most of the data of the present study locate in the transition period of decay:  $n$  is around 6/5 when  $Re_\lambda$  is close to  $O(10^2)$  and it is larger than 6/5 when  $Re_\lambda$  is close to  $O(10)$  and  $O(1)$ . The increasing trend of  $n$  with decreasing  $Re_\lambda$  is in good agreement with previous studies. However, it cannot be concluded whether the present grid turbulence is of Saffman or Batchelor type or neither since the present grid turbulence is in the transition period of decay region.<sup>20</sup> Interestingly, it seems that the behaviors of  $n$  vs  $Re_\lambda$  in previous and present studies have different growing trends from EDQNM. When  $Re_\lambda$  is close to  $O(10^2)$ , most of the data are

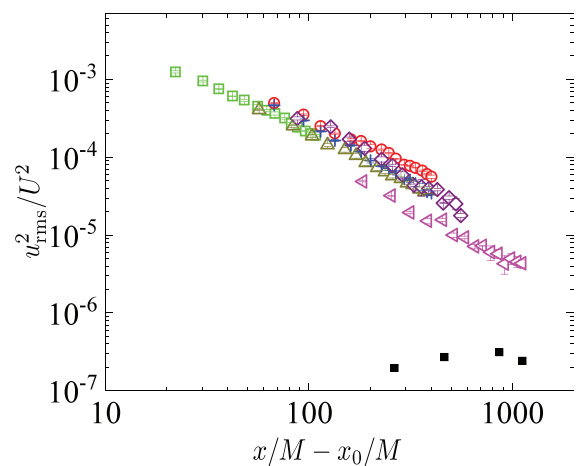


FIG. 2. Decay of turbulent intensity with streamwise distance from a virtual origin  $x_0$ . For symbols, see Table II. Black-square plots refer to background turbulent intensity (measured at  $U_0 = 2$  m/s in the absence of grids).



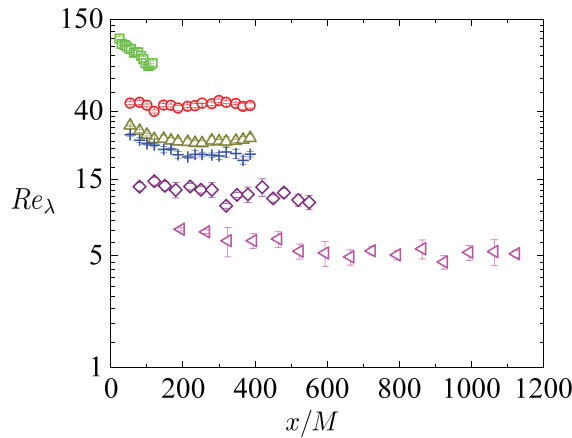


FIG. 3. Streamwise variations of  $Re_\lambda$ . For symbols, see Table II.

close to 6/5 for Saffman turbulence, while at  $Re_\lambda \sim O(10)$ , they are close to Batchelor type estimated by EDQNM. Thus, further investigations of both initial and final periods of decay are necessary for investigating the type of grid turbulence.

### B. Dissipation characteristics

Figure 5 shows the dependence of  $C_\varepsilon = \varepsilon L / u_{\text{rms}}^3$  on  $Re_\lambda$ . The data are compared with previous studies. Here,  $C_\varepsilon$  is calculated assuming isotropy by

$$\varepsilon = 15\nu \overline{\left(\frac{\partial u}{\partial x}\right)^2} = 15\nu \int_0^\infty k_1^2 E_{11}(k_1) dk_1, \quad (10)$$

where  $k_1$  and  $E_{11}(k_1)$  are the one-dimensional wavenumber and one-dimensional energy spectrum, respectively, and the integral length scale by  $L = \frac{E_{11}(k_1=0)\bar{U}}{4u_{\text{rms}}^2}$ .<sup>48</sup> Similar results of  $C_\varepsilon$  are obtained using  $L$

calculated by  $L = \int_0^\infty f(r) dr$ . The dashed and dashed-dotted lines show the theoretical results for stationary HIT given by Lohse,<sup>15</sup> while the solid line shows the DNS result of McComb *et al.* for decaying HIT with their initial spectrum A.<sup>5</sup> Note that the dependence of  $C_\varepsilon$  on the initial spectrum is small in their DNS. Both of the two previous studies provide  $C_\varepsilon$  at  $Re_\lambda \sim O(1)$ , whose reports have not given by experimental studies. Apparently, in the present study when  $Re_\lambda$  is close to  $O(10^2)$ ,  $C_\varepsilon \approx 1$  and this is consistent with the previous studies at similar  $Re_\lambda$ . In contrast, at  $Re_\lambda \sim O(10)$ ,  $C_\varepsilon$  gradually increases with decreasing  $Re_\lambda$ . This result also has numerical and experimental evidence of previous studies. In the final stage of the transition period of decay,  $C_\varepsilon$  increases dramatically as  $Re_\lambda$  decreases. The present result provides the same growing trend as theoretical and DNS studies on HIT at low  $Re_\lambda$ , proving that  $C_\varepsilon$  increases continuously in the final period of decay.<sup>5,15,41</sup> At low  $Re_\lambda$ , the nonlinear energy cascade is broken and grid turbulence is under the domination of dissipation due to viscosity.

### C. Spectral characteristics

It is also meaningful to check the spectral characteristics of grid turbulence since the energy transfer across the scales is more distinguishable in the spectral space. The Kolmogorov scale  $\eta = (\nu^3/\varepsilon)^{1/4}$  describes the length scale connected with the dissipative range. In the spectral space, Kolmogorov<sup>10</sup> predicted that the universal energy spectrum exists in the range  $r \ll L$  for sufficiently high  $Re_\lambda$ . In fact, the universal form has been confirmed in various turbulent flows from moderate to high  $Re_\lambda$  (see details in Pope<sup>50</sup>). However, Djenidi *et al.*<sup>51</sup> found through DNS using the lattice Boltzmann method that the universal form breaks down when  $Re_\lambda$  drops below about 20 in grid turbulence. Note that the universal form has been confirmed for  $Re_\lambda > 23$  in Pope.<sup>50</sup> In the present study, the scaled energy spectrum  $E_{11}(k_1)(\varepsilon\nu^5)^{(-1/4)}$  as a function of  $k_1\eta$  is experimentally examined to explore whether the Kolmogorov's theory is established at low  $Re_\lambda$  or not. Figure 6 shows the normalized one-dimensional longitudinal spectra together with those in previous grid-turbulence experiments.<sup>2</sup> In Fig. 6(a), the inertial subrange  $E_{11}(k_1) \propto k_1^{-5/3}$  can be clearly seen

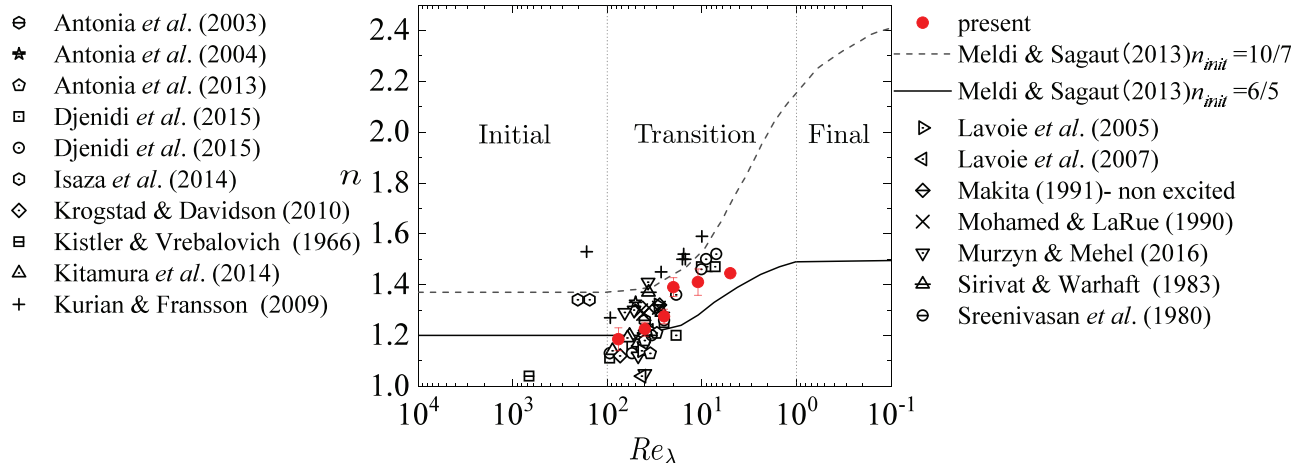
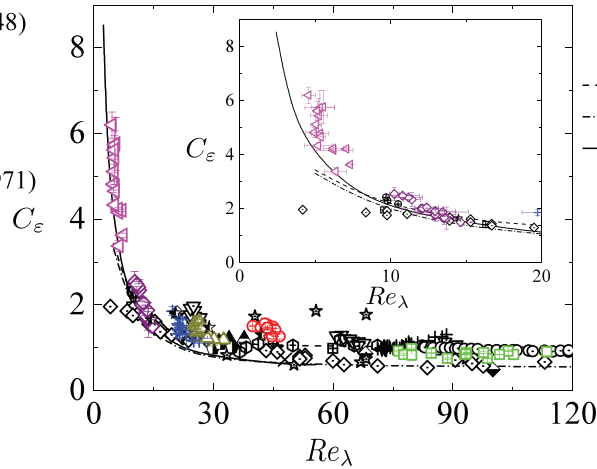


FIG. 4. Variations of the decay exponent  $n$  with  $Re_\lambda$ , shown together with EDQNM<sup>30</sup> and experiments of grid turbulence,<sup>2,4,12,20,27–29,31–38</sup> following Djenidi *et al.*<sup>20</sup> Some of the previous data have been compiled by Antonia *et al.*<sup>13</sup> and Djenidi *et al.*<sup>20</sup>



- ★ Batchelor & Townsend (1948)
- ⊕ Bennet & Corrsin (1978)
- ◇ Bos *et al.* (2007)
- ★ Burattini *et al.* (2005)
- × Burattini *et al.* (2006)
- ⊕ Comte-Bellot & Corrsin (1971)
- ⊞ Djenidi *et al.* (2017)



- ▽ Kitamura *et al.* (2014)
- + Krogstad & Davidson (2010)
- Lohse (1994),  $b = 6$
- Lohse (1994),  $b = 9$
- McComb *et al.* (2010)
- ⊕ Mills *et al.* (1958)
- △ Sreenivasan *et al.* (1980)
- Valente & Vassilicos (2011)
- ◆ Wang *et al.* (1996)

**FIG. 5.** Dependence of  $C_\epsilon$  on  $Re_\lambda$  together with previous studies<sup>1,2,5,15,18,28,38–47</sup> including results for HIT. Some of the previous data have been compiled by Sreenivasan.<sup>45</sup> For symbols used in the present study, see Table II.

only at  $Re_\lambda \sim O(10^2)$ . The compensated energy spectra  $k_1^{5/3} E_{11}(k_1)/\epsilon^{2/3}$  in Fig. 6(b) also confirm this with an approximate plateau at  $Re_\lambda \sim O(10^2)$ . For  $k_1\eta > 0.3$ , the energy spectra deviate from a single curve, which proves the breakdown of Kolmogorov's theory at low  $Re_\lambda$ . Thus, the present study supports the DNS results of

Djenidi *et al.*,<sup>51</sup> which showed the departure of the scaled energy spectrum from those at higher  $Re_\lambda$ .

#### D. Kolmogorov 4/5 law

For HIT at sufficiently high turbulent Reynolds numbers, Kolmogorov<sup>52</sup> derived an exact solution of the third-order structure function, which is known as the 4/5 law

$$\overline{(\delta u(r))^3} = -\frac{4}{5}\epsilon r, \quad (11)$$

$$\overline{\delta u(r)} = \overline{[u(x+r)\bar{u}(x)]}, \quad (12)$$

where  $\delta u$  is the streamwise velocity increment at  $r$ . The 4/5 law is broadly used to investigate the dissipation rate of TKE in real space.<sup>49,53–55</sup> The distributions of  $-(\delta u(r))^3/\epsilon r$  as a function of  $r/\eta$  are shown in Fig. 7. The present results are consistent with Antonia *et al.*<sup>49</sup> at similar turbulent Reynolds numbers, proving good estimations of dissipation rate of TKE in the present study. Deviations from 4/5 law increase with decreasing  $Re_\lambda$ , and none of distributions of  $-(\delta u(r))^3/\epsilon r$  reaches 4/5 although  $-(\delta u(r))^3/\epsilon r$  at  $Re_\lambda \sim O(10^3)$  in Antonia *et al.*<sup>49</sup> is close to 4/5. The present results at lower  $Re_\lambda$  than in

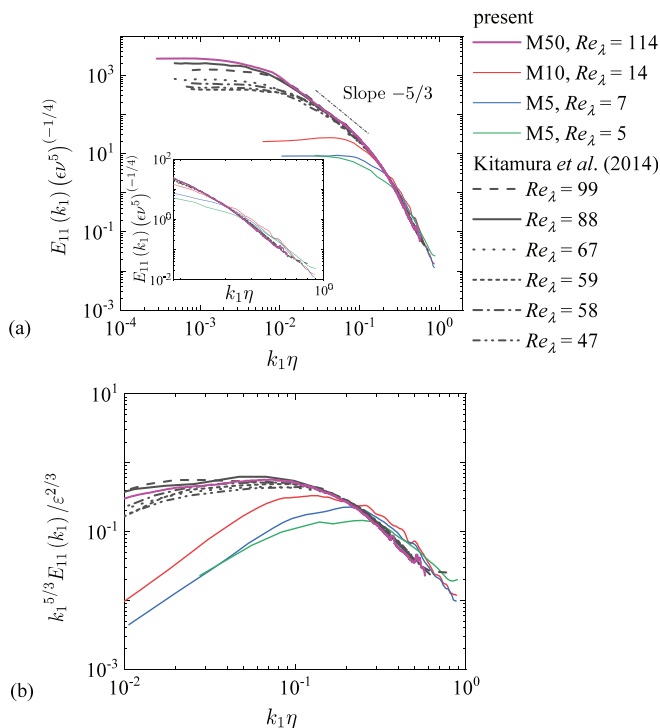


**FIG. 6.** (a) Normalized one-dimensional longitudinal spectra. (b) The compensated energy spectra  $k_1^{5/3} E_{11}(k_1)/\epsilon^{2/3}$ . The present results are compared with previous grid-turbulence experiments at moderate  $Re_\lambda$ .<sup>2</sup>

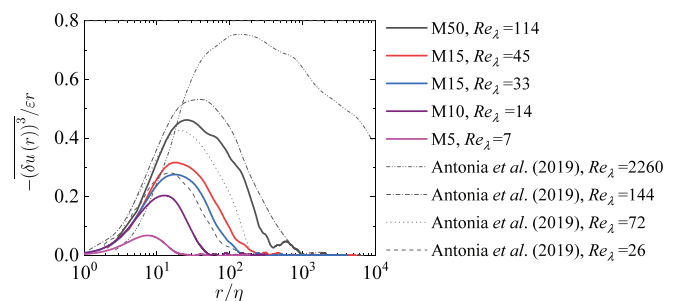


**FIG. 7.** Distributions of  $-(\delta u(r))^3/\epsilon r$  vs  $r/\eta$ , shown together with those in Antonia *et al.*<sup>49</sup>



previous study<sup>49</sup> show the continuous decrease in the peak value of  $-(\delta u(r))^3/\varepsilon r$ .

### E. Variations of quantities related to enstrophy

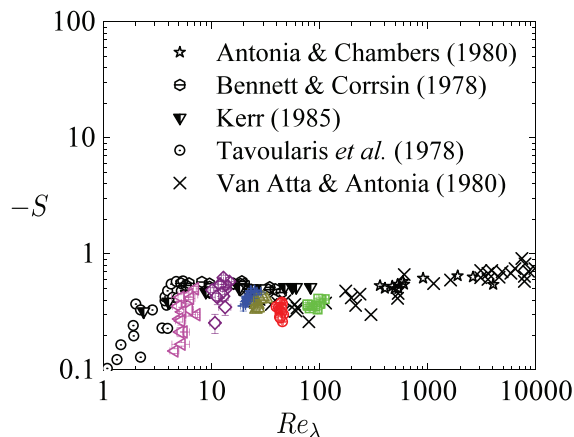
To demonstrate the small-scale characteristics of grid turbulence,  $Re_\lambda$  variations of the velocity derivative skewness  $S$  and flatness  $F = (\partial u/\partial x)^4/[(\partial u/\partial x)^2]^2$  are measured. Kolmogorov<sup>22</sup> proposed that  $S$  and  $F$  differ from 0 and 3 for Gaussian distribution if the small-scale intermittency exists. Sreenivasan and Antonia<sup>56</sup> further confirmed this and compared  $S$  and  $F$  among different experimental data. Figure 8 gives the results of  $-S$  in different turbulent flows. In previous experiments and numerical results,  $S$  departs from 0, rapidly increases at very low  $Re_\lambda$  (Tavoularis *et al.*<sup>23</sup>) exhibits a plateau at moderate  $Re_\lambda$  (Bennett and Corrsin,<sup>18</sup> Kerr,<sup>24</sup>) and finally slightly increases as  $Re_\lambda$  increases (Van Atta and Antonia,<sup>25</sup> Antonia and Chambers<sup>26</sup>). The behavior of the present result of  $-S$  agrees well with previous studies. Besides, the growing extent of  $-S$  in M5 case varies from nearly 0.1 to 0.6, while  $-S$  in M50 is nearly constant. This result suggests that  $-S$  decreases with longer streamwise distance while the variation of  $Re_\lambda$  is small, and the nonlinear force in the K–H equation/production of enstrophy is getting smaller at very low  $Re_\lambda$ .

Figure 9 shows the present and previous experimental data of  $F$  vs  $Re_\lambda$ . In Fig. 9, the present data remain almost constant and most of them locate between 3 and 4, which are consistent with previous data of the same range of  $Re_\lambda$ .

Figure 10 shows  $G/Re_\lambda$  as functions of  $Re_\lambda$ . As grid turbulence decays according to a power law, Eq. (5) can be deduced to the form<sup>57</sup>

$$\frac{G}{Re_\lambda} = \frac{15(n+1)}{7nRe_\lambda} - \frac{1}{2}S. \quad (13)$$

Note that Eq. (13) has been derived assuming HIT and neglecting turbulent and viscous diffusions of vorticity.<sup>57</sup> The present data of  $G/Re_\lambda$  are in good agreement with previous experimental data at high  $Re_\lambda$ . On the other hand,  $G/Re_\lambda$  increases dramatically in the final stage of



**FIG. 8.** Relationship between the velocity derivative skewness  $-S$  and  $Re_\lambda$ . The present results are compared with theoretical analysis,<sup>25</sup> experiments of grid turbulence,<sup>18,23</sup> atmospheric flows,<sup>26</sup> and numerical results.<sup>24</sup> For symbols used in the present study, see Table II. Part of the previous data have been compiled by Sreenivasan and Antonia.<sup>56</sup>

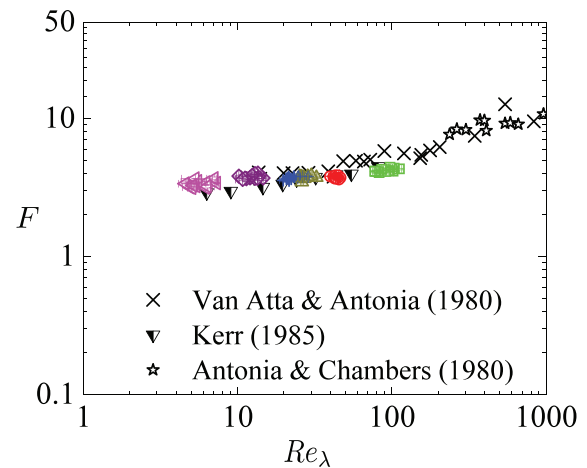


**FIG. 9.** Relationship between the velocity derivative flatness  $F$  and  $Re_\lambda$ . Data from different sources<sup>24–26</sup> have been compiled by Sreenivasan and Antonia.<sup>56</sup> For symbols used in the present study, see Table II.

the transition period of decay. It can be seen that the variation of  $G/Re_\lambda$  with  $Re_\lambda$  can be fitted well with a power law even at very low  $Re_\lambda$  using different  $n$  and  $S$  in different period of decay. Note that present results cover smaller value of  $Re_\lambda$ , i.e., larger value of  $G/Re_\lambda$  than in previous studies.<sup>58,59</sup>

Finally, to further investigate the variations of enstrophy in the decay process of grid turbulence, Fig. 11 shows the relationship between  $S + 2G/Re_\lambda$  and  $Re_\lambda$ . The dashed line is the nonlinear fit using the least squares method with a power-law exponent of  $-1.09$ . When  $Re_\lambda > 60$ ,  $S + 2G/Re_\lambda$  is close to zero, while  $S + 2G/Re_\lambda$  rapidly increases and reaches nearly 2 at very low  $Re_\lambda$  following a power law. In other words, the enstrophy decreases in the whole decay process due to the viscosity at low  $Re_\lambda$ . There exists an imbalance between production and destruction of enstrophy, and the imbalance becomes significant at very low  $Re_\lambda$ . This result and power-law fitting strongly support that the prospection of this imbalance follows an exponential increase from the transition to the final period of decay. Note that as in Fig. 10, present results cover smaller value of  $Re_\lambda$ , i.e., larger value of

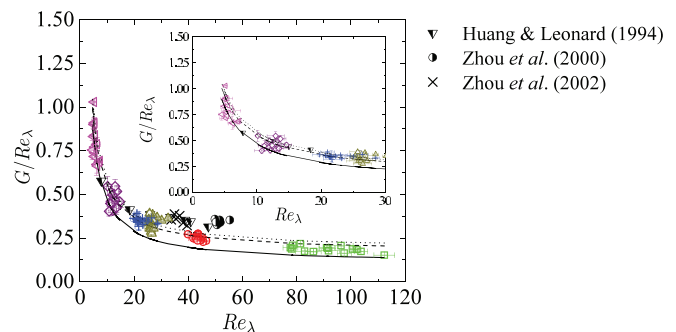


**FIG. 10.** Variations of  $G/Re_\lambda$  with  $Re_\lambda$ . Previous data<sup>60–62</sup> have been compiled by Djenidi and Antonia<sup>57</sup> and Lee *et al.*<sup>59</sup> The lines are calculated with Eq. (13): solid,  $n = 1.45$ ,  $S = -0.21$ ; dashed,  $n = 1.28$ ,  $S = -0.34$ ; dot,  $n = 1.17$ ,  $S = -0.37$ . For symbols used in the present study, see Table II.



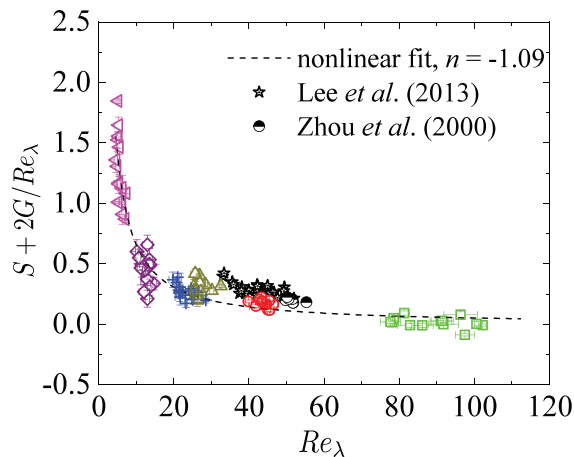


FIG. 11. Variations of  $S + 2G/Re_\lambda$  with  $Re_\lambda$ . The dashed line represents a nonlinear fit of present data. For symbols used in the present study, see Table II.

$S + 2G/Re_\lambda$  than in previous studies. The ratio of production and destruction,  $\frac{-S}{2G/Re_\lambda}$ , is shown in Fig. 12. At moderate  $Re_\lambda$ , production and destruction terms are almost the same in magnitude. The ratio decreases as  $Re_\lambda$  decreases and the destruction of vorticity becomes dominant at low  $Re_\lambda$ .

#### IV. CONCLUSIONS

The study of decaying HIT with extremely high or low  $Re_\lambda$  is still charming since the turbulence theories of HIT at these specific ranges of  $Re_\lambda$  are lacking experimental evidence. In this study, velocity measurements in grid turbulence are conducted up to far downstream region of  $x/M \sim O(10^3)$  and  $Re_\lambda \sim O(1)$ . The energy decay characteristics and turbulent quantities related to enstrophy variations of grid turbulence are measured for four grids (square grid with mesh sizes  $M = 10, 15$ , and  $50$  mm and woven-mesh grid with a mesh size  $M = 5$  mm) and six mesh Reynolds numbers ( $Re_M = 680, 1300, 5800, 9600$ , and  $33\,000$ ).

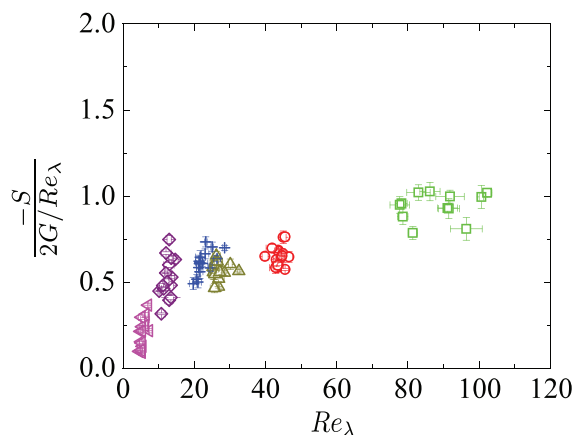


FIG. 12. Variations of  $\frac{-S}{2G/Re_\lambda}$  with  $Re_\lambda$ . For symbols, see Table II.

For the energy decay of grid turbulence, although the power-law decay exponent  $n$  at rather high  $Re_\lambda$  is close to  $6/5$  for Saffman turbulence, it is difficult to justify whether grid turbulence at the transition period of decay is still Saffman turbulence or not as already suggested by Djenidi *et al.*<sup>20</sup> However, an interesting observation is that  $n$  is close to  $6/5$  for Saffman turbulence at moderate  $Re_\lambda$  but it becomes close to the value for Batchelor turbulence predicted by EDQNM as  $Re_\lambda$  decreases. This possible change, if correct, should be further investigated with much lower  $Re_\lambda$  than in present study, i.e., in the final period of decay region. It is well known that the universal energy spectrum exists in the range  $r \ll L$  at sufficiently high  $Re_\lambda$ . However, the one-dimensional energy spectra in the dissipation range at low  $Re_\lambda$  deviate from the universal form, in agreement with previous DNS on grid turbulence.

$C_\epsilon$ ,  $G$ , and  $S + 2G/Re_\lambda$  increase dramatically as  $Re_\lambda$  decreases in the final stage of the transition period of decay. The present study covers the smaller value of  $Re_\lambda$  than in previous study and offers the experimental evidence of continuous increase in the effect of viscosity on dissipation of TKE and in enstrophy destruction due to viscosity in the final stage of the transition period of decay. The growing trend of  $S + 2G/Re_\lambda$  has well prospected with a power law with an exponent  $-1.09$  even in the final stage of the transition period of decay.

In conclusion, the present study demonstrates that the nonlinear energy cascade is well established at rather high  $Re_\lambda$  and predictions by previous DNS and theories at very low  $Re_\lambda$  are justified by the present experiments. The investigations of extremely low  $Re_\lambda$  (i.e., from final stage of the transition period of decay to the final period of decay) are necessary for the future work.

#### ACKNOWLEDGMENTS

The authors would like to thank Mr. Tetsuya Matsushima (Nagoya University) for his cooperation in conducting the experiments. This study is supported by the JSPS KAKENHI, Grant No. 18H01367. The first author was financially supported by the DII collaborative Graduate Program for Accelerating Innovation in Future Electronics, Nagoya University.

#### DATA AVAILABILITY

The data that support the findings of this study are available from the corresponding author upon reasonable request.

#### REFERENCES

- G. K. Batchelor and A. A. Townsend, "Decay of turbulence in the final period," *Proc. R. Soc. A* **194**, 527 (1948).
- T. Kitamura, K. Nagata, Y. Sakai, A. Sasoh, O. Terashima, H. Saito, and T. Harasaki, "On invariants in grid turbulence at moderate Reynolds numbers," *J. Fluid Mech.* **738**, 378 (2014).
- G. K. Batchelor and A. A. Townsend, "Decay of vorticity in isotropic turbulence," *Proc. R. Soc. A* **190**, 534 (1947).
- P. Lavoie, L. Djenidi, and R. A. Antonia, "Effects of initial conditions in decaying turbulence generated by passive grids," *J. Fluid Mech.* **585**, 395 (2007).
- W. D. McComb, A. Berera, M. Salewski, and S. Yoffe, "Taylor's (1935) dissipation surrogate reinterpreted," *Phys. Fluids* **22**, 061704 (2010).
- T. V. Kármán, "The fundamentals of the statistical theory of turbulence," *J. Aeronaut. Sci.* **4**, 131 (1937).
- T. de Kármán and L. Howarth, "On the statistical theory of isotropic turbulence," *Proc. R. Soc. A* **164**, 192 (1938).
- H. Tennekes and J. L. Lumley, *A First Course in Turbulence* (MIT Press, 2018).



- <sup>9</sup>J. C. Vassilicos, "Dissipation in turbulent flows," *Annu. Rev. Fluid Mech.* **47**, 95 (2015).
- <sup>10</sup>A. N. Kolmogorov, "On degeneration (decay) of isotropic turbulence in an incompressible viscous liquid," *Dokl. Akad. Nauk SSSR* **31**, 538 (1941).
- <sup>11</sup>P. G. Saffman, "The large-scale structure of homogeneous turbulence," *J. Fluid Mech.* **27**, 581 (1967).
- <sup>12</sup>M. S. Mohamed and J. C. LaRue, "The decay power law in grid-generated turbulence," *J. Fluid Mech.* **219**, 193 (1990).
- <sup>13</sup>R. A. Antonia, S. K. Lee, L. Djenidi, P. Lavoie, and L. Danaila, "Invariants for slightly heated decaying grid turbulence," *J. Fluid Mech.* **727**, 379 (2013).
- <sup>14</sup>G. K. Batchelor, *The Theory of Homogeneous Turbulence* (Cambridge university Press, 1953).
- <sup>15</sup>D. Lohse, "Crossover from high to low Reynolds number turbulence," *Phys. Rev. Lett.* **73**, 3223 (1994).
- <sup>16</sup>G. K. Batchelor and A. A. Townsend, "Decay of isotropic turbulence in the initial period," *Proc. R. Soc. A* **193**, 539 (1948b).
- <sup>17</sup>G. K. Batchelor and I. Proudman, "The large-scale structure of homogenous turbulence," *Philos. Trans. R. Soc., A* **248**, 369 (1956).
- <sup>18</sup>J. C. Bennett and S. Corrsin, "Small Reynolds number nearly isotropic turbulence in a straight duct and a contraction," *Phys. Fluids* **21**, 2129 (1978).
- <sup>19</sup>L. Skrbek and S. R. Stalp, "On the decay of homogeneous isotropic turbulence," *Phys. Fluids* **12**, 1997 (2000).
- <sup>20</sup>L. Djenidi, M. Kamruzzaman, and R. A. Antonia, "Power-law exponent in the transition period of decay in grid turbulence," *J. Fluid Mech.* **779**, 544 (2015).
- <sup>21</sup>G. I. Taylor, "Production and dissipation of vorticity in a turbulent fluid," *Proc. R. Soc. A* **164**, 15 (1938).
- <sup>22</sup>A. N. Kolmogorov, "A refinement of previous hypotheses concerning the local structure of turbulence in a viscous incompressible fluid at high Reynolds number," *J. Fluid Mech.* **13**, 82 (1962).
- <sup>23</sup>S. Tavoularis, J. C. Bennett, and S. Corrsin, "Velocity-derivative skewness in small Reynolds number, nearly isotropic turbulence," *J. Fluid Mech.* **88**, 63 (1978).
- <sup>24</sup>R. M. Kerr, "Higher-order derivative correlations and the alignment of small-scale structures in isotropic numerical turbulence," *J. Fluid Mech.* **153**, 31 (1985).
- <sup>25</sup>C. W. Van Atta and R. A. Antonia, "Reynolds number dependence of skewness and flatness factors of turbulent velocity derivatives," *Phys. Fluids* **23**, 252 (1980).
- <sup>26</sup>R. A. Antonia and A. J. Chambers, "On the correlation between turbulent velocity and temperature derivatives in the atmospheric surface layer," *Boundary Layer Meteorol.* **18**, 399 (1980).
- <sup>27</sup>J. Isaza, R. Salazar, and Z. Warhaft, "On grid-generated turbulence in the near- and far field regions," *J. Fluid Mech.* **753**, 402 (2014).
- <sup>28</sup>P.-Å. Krogstad and P. A. Davidson, "Is grid turbulence Saffman turbulence?," *J. Fluid Mech.* **642**, 373 (2010).
- <sup>29</sup>H. Makita, "Realization of a large-scale turbulence field in a small wind tunnel," *Fluid Dyn. Res.* **8**, 53 (1991).
- <sup>30</sup>M. Meldi and P. Sagaut, "Further insights into self-similarity and self-preservation in freely decaying isotropic turbulence," *J. Turbul.* **14**, 24 (2013).
- <sup>31</sup>R. A. Antonia, R. J. Smalley, T. Zhou, F. Anselmet, and L. Danaila, "Similarity of energy structure functions in decaying homogeneous isotropic turbulence," *J. Fluid Mech.* **487**, 245 (2003).
- <sup>32</sup>R. A. Antonia, R. J. Smalley, T. Zhou, F. Anselmet, and L. Danaila, "Similarity solution of temperature structure functions in decaying homogeneous isotropic turbulence," *Phys. Rev. E* **69**, 016305 (2004).
- <sup>33</sup>A. L. Kistler and T. Vrebalovich, "Grid turbulence at large Reynolds numbers," *J. Fluid Mech.* **26**, 37 (1966).
- <sup>34</sup>T. Kurian and J. H. Fransson, "Grid-generated turbulence revisited," *Fluid Dyn. Res.* **41**, 021403 (2009).
- <sup>35</sup>P. Lavoie, P. Burattini, L. Djenidi, and R. A. Antonia, "Effect of initial conditions on decaying grid turbulence at low  $Re_z$ ," *Exp. Fluids* **39**, 865 (2005).
- <sup>36</sup>F. Murzyn and A. Mehel, "Influence of the virtual origin on the turbulent length scales in the grid-generated turbulence," *Int. J. Fluid Mech. Res.* **43**, 62 (2016).
- <sup>37</sup>A. Sirivat and Z. Warhaft, "The effect of a passive cross-stream temperature gradient on the evolution of temperature variance and heat flux in grid turbulence," *J. Fluid Mech.* **128**, 323 (1983).
- <sup>38</sup>K. R. Sreenivasan, S. Tavoularis, R. Henry, and S. Corrsin, "Temperature fluctuations and scales in grid-generated turbulence," *J. Fluid Mech.* **100**, 597 (1980).
- <sup>39</sup>W. J. Bos, L. Shao, and J. P. Bertoglio, "Spectral imbalance and the normalized dissipation rate of turbulence," *Phys. Fluids* **19**, 045101 (2007).
- <sup>40</sup>P. Burattini, P. Lavoie, and R. A. Antonia, "On the normalized turbulent energy dissipation rate," *Phys. Fluids* **17**, 098103 (2005).
- <sup>41</sup>P. Burattini, P. Lavoie, A. Agrawal, L. Djenidi, and R. A. Antonia, "Power law of decaying homogeneous isotropic turbulence at low Reynolds number," *Phys. Rev. E* **73**, 066304 (2006).
- <sup>42</sup>G. Comte-Bellot and S. Corrsin, "Simple Eulerian time correlation of full- and narrow-band velocity signals in grid-generated, 'isotropic' turbulence," *J. Fluid Mech.* **48**, 273 (1971).
- <sup>43</sup>L. Djenidi, N. Lefeuvre, M. Kamruzzaman, and R. A. Antonia, "On the normalized dissipation parameter  $C_\epsilon$  in decaying turbulence," *J. Fluid Mech.* **817**, 61 (2017).
- <sup>44</sup>R. R. Mills, Jr., A. L. Kistler, V. O'Brien, and S. Corrsin, "Turbulence and temperature fluctuations behind a heated grid," NACA Technical Report No. 4288 (1958).
- <sup>45</sup>K. R. Sreenivasan, "On the scaling of the turbulence energy dissipation rate," *Phys. Fluids* **27**, 1048 (1984).
- <sup>46</sup>P. C. Valente and J. C. Vassilicos, "The decay of homogeneous turbulence generated by multi-scale grids," in *Proceedings of the Seventh International Symposium on Turbulence and Shear Flow Phenomena* (Begel House, Inc., 2011).
- <sup>47</sup>L. P. Wang, S. Chen, J. G. Brasseur, and J. C. Wyngaard, "Examination of hypotheses in the kolmogorov refined turbulence theory through high-resolution simulations. I. Velocity field," *J. Fluid Mech.* **309**, 113 (1996).
- <sup>48</sup>P. E. Roach, "The generation of nearly isotropic turbulence by means of grids," *Int. J. Heat Fluid Flow* **8**, 82 (1987).
- <sup>49</sup>R. A. Antonia, S. L. Tang, L. Djenidi, and Y. Zhou, "Finite Reynolds number effect and the 4/5 law," *Phys. Rev. Fluids* **4**, 084602 (2019).
- <sup>50</sup>S. B. Pope, *Turbulent Flows* (IOP Publishing, 2001).
- <sup>51</sup>L. Djenidi, S. F. Tardu, R. A. Antonia, and L. Danaila, "Breakdown of Kolmogorov's first similarity hypothesis in grid turbulence," *J. Turbul.* **15**, 596 (2014).
- <sup>52</sup>A. N. Kolmogorov, "Dissipation of energy in the locally isotropic turbulence," *Dokl. Akad. Nauk SSSR* **32**, 16 (1941).
- <sup>53</sup>A. Paul, P. K. Raushan, S. K. Singh, and K. Debnath, "Organized structure of turbulence in wave-current combined flow over rough surface using spatio-temporal averaging approach," *J. Braz. Soc. Mech. Sci. Eng.* **42**, 1 (2020).
- <sup>54</sup>F. Coscarella, S. Servidio, D. Ferraro, V. Carbone, and R. Gaudio, "Turbulent energy dissipation rate in a tilting flume with a highly rough bed," *Phys. Fluids* **29**, 085101 (2017).
- <sup>55</sup>D. Ferraro, S. Servidio, V. Carbone, S. Dey, and R. Gaudio, "Turbulence laws in natural bed flows," *J. Fluid Mech.* **798**, 540 (2016).
- <sup>56</sup>K. R. Sreenivasan and R. A. Antonia, "The phenomenology of small-scale turbulence," *Annu. Rev. Fluid Mech.* **29**, 435 (1997).
- <sup>57</sup>L. Djenidi and R. A. Antonia, "Transport equation for the mean turbulent energy dissipation rate in low- $Re_z$  grid turbulence," *J. Fluid Mech.* **747**, 288 (2014).
- <sup>58</sup>T. Zhou and R. A. Antonia, "Reynolds number dependence of the small-scale structure of grid turbulence," *J. Fluid Mech.* **406**, 81 (2000).
- <sup>59</sup>S. K. Lee, L. Djenidi, R. A. Antonia, and L. Danaila, "On the destruction coefficients for slightly heated decaying grid turbulence," *Int. J. Heat Fluid Flow* **43**, 129 (2013).
- <sup>60</sup>M. J. Huang and A. Leonard, "Power-law decay of homogeneous turbulence at low Reynolds numbers," *Phys. Fluids* **6**, 3765 (1994).
- <sup>61</sup>T. Zhou, R. A. Antonia, L. Danaila, and F. Anselmet, "Transport equations for the mean energy and temperature dissipation rates in grid turbulence," *Exp. Fluids* **28**, 143 (2000).
- <sup>62</sup>T. Zhou, R. A. Antonia, and L. P. Chua, "Performance of a probe for measuring turbulent energy and temperature dissipation rates," *Exp. Fluids* **33**, 334 (2002).